
This is an electronic reprint of the original article.
This reprint may differ from the original in pagination and typographic detail.

Author(s): Ganchenkova, M. G. & Kuznetsov, A. Yu. & Nieminen, Risto M.
Title: Electronic structure of the phosphorus-vacancy complex in silicon: A resonant-bond model
Year: 2004
Version: Final published version

Please cite the original version:

Ganchenkova, M. G. & Kuznetsov, A. Yu. & Nieminen, Risto M. 2004. Electronic structure of the phosphorus-vacancy complex in silicon: A resonant-bond model. *Physical Review B*. Volume 70, Issue 11. 115204/1-11. ISSN 1550-235X (electronic). DOI: 10.1103/physrevb.70.115204.

Rights: © 2004 American Physical Society (APS). This is the accepted version of the following article: Ganchenkova, M. G. & Kuznetsov, A. Yu. & Nieminen, Risto M. 2004. Electronic structure of the phosphorus-vacancy complex in silicon: A resonant-bond model. *Physical Review B*. Volume 70, Issue 11. 115204/1-11. ISSN 1550-235X (electronic). DOI: 10.1103/physrevb.70.115204, which has been published in final form at <http://journals.aps.org/prb/abstract/10.1103/PhysRevB.70.115204>.

All material supplied via Aaltodoc is protected by copyright and other intellectual property rights, and duplication or sale of all or part of any of the repository collections is not permitted, except that material may be duplicated by you for your research use or educational purposes in electronic or print form. You must obtain permission for any other use. Electronic or print copies may not be offered, whether for sale or otherwise to anyone who is not an authorised user.

Electronic structure of the phosphorus-vacancy complex in silicon: A resonant-bond model

M. G. Ganchenkova

Laboratory of Material Physics and Semiconductors, Royal Institute of Technology, Isafjordsgatan 22, P.O. Box Electrum 229, SE-164 40 Kista, Sweden

A. Yu. Kuznetsov

Laboratory of Physical Electronics, Department of Physics, University of Oslo, P.O. Box 1048-Blindern, 0316 Oslo, Norway

R. M. Nieminen

COMP/Laboratory of Physics, Helsinki University of Technology, P.O. Box 1100, 02015 Espoo, Finland

(Received 16 November 2003; published 9 September 2004)

Using first-principles calculations, the electronic structure of the phosphorus-vacancy pair in silicon has been studied. Detailed analysis of the atomic displacement fields associated with the atomic structure optimization after the defect formation indicates a strong dependence of the character and magnitude of relaxation both on the supercell size and the E-center charge state. Our simulation results strongly suggest that the E-center structure is of the resonant-bond type with a strong localization of an electron pair at the phosphorus atom. The energy level splitting for shared electrons in a vacancy due to the appearance of the resonance distortion is discussed, as well as the nature of and the reasons for the level occupation.

DOI: 10.1103/PhysRevB.70.115204

PACS number(s): 61.72.-y, 71.20.-b, 71.55.-i

I. INTRODUCTION

Investigations of energetics, atomic structure, and electronic properties of dopant atoms and intrinsic point defects in silicon have been for a long time an issue attracting attention of the research community dealing with electronics materials. The reason is evident: efficient performance of basic electronic devices (e.g., diodes and transistors) is provided by the possibility to affect the conductivity type of the same material by controlled addition of appropriate dopants. Reliable control of inhomogeneous doping profiles, as demanded by current trends in microelectronics technologies, requires a detailed knowledge of the properties not only of dopants (in silicon technology the most important ones are phosphorus and boron), but also of intrinsic point defects, especially-vacancies (V), and different dopant-defect complexes. However, in spite of the progress in elucidation of point defect diffusion and dopant-defect interaction mechanisms in silicon, many open questions remain. For example, the knowledge of electronic and diffusion characteristics of intrinsic defects and dopants in *n*-doped silicon is still far from complete, regardless of the fact that this material is particularly important for many technological applications.

The structure and electronic properties of individual vacancies and divacancies in Si are among those studied most extensively, starting from the pioneering works of Watkins and Corbett.^{1,2} Even these rather simple defects have demonstrated, however, quite a nontrivial behavior, which remains still a source of controversy. Let us consider, for example, the relaxation pattern of atoms surrounding vacancies and divacancies. In metals, where the interatomic distances are usually smaller than the position of minimum of the pair potential (due to long range attractive interaction), an inward relaxation of the nearest vacancy neighbors is typically observed. However, in covalent crystals, such as silicon, the interatomic bonds are short-ranged and the perfect lattice is

not internally strained. In such a situation, the degree and even the direction of the first neighbor shell relaxation around a vacancy is strongly determined by interaction of dangling bonds from the vacancy neighbors and can hardly be predicted ad hoc. As follows from the recent calculations for the vacancy and divacancy,^{3,4} an inward relaxation for the defect nearest environment is expected in these cases, which is most probably related to the strong interaction of dangling interatomic bonds in a vacancy.

Indeed, the energy penalty for having four unpaired bonds is so high that pairwise bonding of silicon of a vacancy is energetically favorable regardless of the elastic distortion of the vacancy neighborhood. Thus a reduction of symmetry accompanies the vacancy formation. As first pointed out in Ref. 2, this distortion is a specific manifestation of the well-known Jahn-Teller effect.⁵ The model of Jahn-Teller distortion, proposed by Watkins and Corbett to interpret their electron spin resonance (ESR) experiments² is considered now to be commonly accepted. However, already for the divacancy the situation is much less unequivocal. In fact, the same kind of interatomic bonding was proposed to describe Jahn-Teller distortion in silicon divacancies.⁶ The pairing distortion model complied with the predictions of both the EPR measurements and the experiments on electron nuclear double resonance (ENDOR) (Ref. 7) and for a long time this bonding model was the only one considered. However, *ab initio* calculations by Saito and Oshiyama⁸ have demonstrated a completely different type of Jahn-Teller distortion in this case related to a different type of dangling bond pairing. Indeed, in contrast to weak covalent bonds that provide the pairing distortion in a vacancy, resonant bonds between divacancy neighbors are formed, providing the same type of symmetry reduction, as indicated by earlier experiments, but requiring a much weaker elastic distortion of the vacancy surroundings.

A much more complicated situation occurs, when a vacancy in silicon forms a complex with a substitutional dopant atom. The phosphorus–vacancy pair (PV or E-center) is the main interest for our current consideration. In their study of neutral PV-pairs in silicon, Watkins and Corbett⁷ adopted the model of the same weak covalent bonding as in a vacancy and a divacancy, which allowed reasonable rationalization of electron paramagnetic resonance (EPR) observations. In particular, the experimental data indicated that the phosphorus atom has all its orbitals completely filled and is not bonded to the other vacancy neighbors. As a result, only one weak covalent bond between two (arbitrary) Si atoms neighboring the vacancy was postulated, while the remaining Si atom was assumed to have a dangling orbital pointing towards the vacant site. However, the same symmetry can be equally well described by two alternative models (weak covalent or resonant bonding), neither of which can be definitely rejected on the basis of the available experimental results. The situation with the distortion patterns associated with the E-center can be even more complicated, because it can be not only neutral, as studied in the EPR experiments,⁷ but also charged, either positively or negatively. In fact, even a relaxation direction for the first neighbors of a vacancy in the E-center remains uncertain. To our knowledge, during the last 15 years only a few theoretical and experimental studies were performed to clarify this uncertainty. In particular, deep-level-transient spectroscopy (DLTS) was used by Samara⁹ to study lattice relaxation accompanying electron capture by the complex and estimate the deep level positions associated with it. These DLTS results indicate the shrinkage of the E-center in the transition from neutral to negative charge state. Later positron life time experiments by Mäkinen *et al.*^{10,11} confirmed the inward relaxation associated with this kind of charge transition. These findings are in agreement with molecular dynamics simulation,¹² based on the Car-Parrinello approach,¹³ which also shows the inward relaxation of the first neighbor shell of a vacancy. However, the interpretation¹⁴ of the positron lifetime experiment^{10,11} favors outwards relaxation for neutral and negatively charged E-centers. It should be noted, however, that very similar positron lifetime predictions indicate outwards relaxation also for the first neighbors of vacancies and divacancies in bulk, Si,¹⁵ where all recent calculations^{3,4} agree about the inward relaxation pattern.

Having in mind the uncertain current state of the art with the structural relaxation and bonding configurations of phosphorus-vacancy complexes in Si, we address in this paper the main features of the atomic and electronic structure optimization of the E-center, as well as the energetic parameters of the defect for three charge states (PV^+ , PV^0 , and PV^-). All calculations have been performed in the framework of the density-functional theory within the local-(spin)-density approximation. The details of the simulation technique and convergence tests are presented in Sec. II. A detailed analysis of the displacement fields associated with the structure optimization of the defect is given in Sec. III A, while the electronic structure is described in Sec. III B. In particular, our simulation results strongly suggest that the E-center structure is of the resonant-bond type with a strong localization of an electron pair on the phosphorus atom. The

TABLE I. The relaxations for the nearest neighbors of a PV complex in its different charge states calculated using different approximations (LDA and LSDA), cutoff energies. Pd and Vd are distance between nearest neighbors of the P atom and vacancy, respectively (Fig. 1). The values of distances are presented in Å, of cutoff energies are presented in eV.

(P-V) ⁰		Pd1	Pd2	Pd3	Vd1	Vd2	Vd3
150.544	LSDS	3.71	3.71	3.71	3.49	3.49	3.49
	LDA	3.71	3.71	3.71	3.49	3.49	3.49
173.298	LDA	3.71	3.71	3.71	3.51	3.51	3.51
216.623	LDA	3.71	3.71	3.71	3.51	3.51	3.51
(P-V) ⁻		Pd1	Pd2	Pd3	Vd1	Vd2	Vd3
150.544	LSDA	3.71	3.71	3.71	3.36	3.36	3.36
	LDA	3.71	3.71	3.71	3.36	3.36	3.36
173.298	LSDA	3.71	3.71	3.71	3.36	3.36	3.36
216.623	LSDA	3.71	3.71	3.71	3.38	3.38	3.38
(P-V) ⁺		Pd1	Pd2	Pd3	Vd1	Vd2	Vd3
150.544	LSDA	3.72	3.72	3.72	3.63	3.63	3.63
	LDA	3.71	3.71	3.71	3.63	3.63	3.63
173.298	LSDA	3.72	3.72	3.72	3.63	3.63	3.63
216.623	LSDA	3.72	3.72	3.72	3.64	3.64	3.64

energy level splitting for the shared electrons in the vacancy due to the appearance of the resonant distortion, as well as the nature of and the reasons for the level occupation are discussed in Sec. IV. Finally, the concluding section summarizes the main results obtained.

II. SIMULATION DETAILS

The calculations have been performed using the plane wave basis VASP code implementing both the local density approximation (LDA) and the local spin-density approximation (LSDA). We use the ultrasoft Vanderbilt pseudopotentials to represent the core electrons. All defect calculations were made using either $2 \times 2 \times 2$ (64 atoms) or $3 \times 3 \times 3$ (216 atoms) atomic unit cells with periodic boundary conditions. Brillouin zone sampling of the charge density was done using the (2,2,2) Monkhorst-Pack parameters. The atoms were allowed to relax until the Hellmann-Feynman forces were less than $0.003 \text{ eV}/\text{Å}^3$.

For the overall consistency of results, it is important to appropriately select the cutoff energy and the type of local density approximation. First of all, we have investigated the convergence of the formation energy value and relaxation displacements values with respect to the cutoff energy. Three different values of the cutoff energy were considered, including the standard values of the Vanderbilt potential for silicon (150.544 eV) and for phosphorus (173.298 eV). As can be seen in Table I, the formation energies and the distances between the nearest neighbors of a PV pair (see below for

TABLE II. Shifts of phosphorus atom that are result of structure optimization after formation of a PV complex, as a fraction of the interatomic distance in pure Si (in %) SC stands for supercell.

Complex	64 SC	216 SC
PV ⁺	0.71	1.95
PV ⁰	2.29	3.30
PV ⁻	2.84	3.68

details) are practically insensitive to the choice of the cutoff energy. For this reason, in our calculations we used the cutoff energy of 150.544 eV.

Secondly, as the defect has an odd number of electrons, it may be more appropriate to apply spin-polarized DFT in the local-spin-density approximation.¹⁶ However, LSDA calculations require double CPU time. Therefore, the sensitivity of the results to the approximation type was checked by parallel calculations with both LD and LSD approximations for a 64 atom supercell (SC). As shown in Table I, for all charge states of a PV complex the values obtained using different approximations are practically the same. For this reason, in a bigger supercell with 216 atoms the task was performed in two steps: (i) basic relaxation of the ensemble (both ionic and electronic systems) using LDA and (ii) additional relaxation using LSDA.

III. CALCULATION RESULTS

A. Relaxation of atoms around the PV complex

To create an E-center, two adjacent silicon atoms were removed and one of the formed vacant positions was filled with a phosphorus atom in the silicon lattice. After that the system was numerically relaxed. The resulting symmetry of the atomic configuration of the defect was found insensitive to the choice of density functional approximation (LDA or LSDA). On the other hand, the charge state of the defect influences the relaxation pattern significantly.

After the relaxation, the phosphorus atom shifts from the initial lattice site strictly in the direction of the vacant site. The shifts are quite small (0.02–0.09 Å), and the smallest one corresponds to positively charged complex PV⁺. As can be seen in Table II, the addition of one electron to this complex (i.e., the pair PV⁰) provides quite noticeable additional shift of the P atom towards the vacancy. However, an addition of the second electron (resulting in PV⁻) contributes to the shift much less.

A similar tendency can be seen for the atoms surrounding the complex (the nearest neighbors). There are six atoms in the first coordination shell of the PV complex, which can be conveniently separated in two groups, depending on their proximity either to the vacancy or to the phosphorus atom (Fig. 1). The relaxation of atoms in these groups is pronouncedly different.

In particular, the symmetry of the group of atoms near the vacancy (marked in Fig. 1 as SiV_j, where $j=1,2,3$) was found to be sensitive to the size of the supercell. In the case of a 64-atom SC the atomic triangle relaxes symmetrically

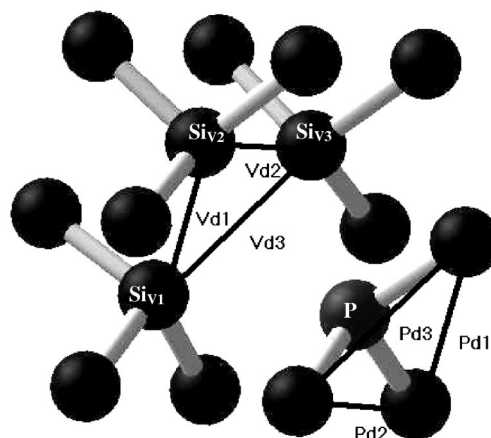


FIG. 1. Schematics of the atomic structure of the first coordination shell around a PV complex.

towards the vacant site and the distances between the atoms in the group decrease as compared to those in the bulk Si (see Table III), but remain equal to each other (e.g., $V_{d1} = V_{d2} = V_{d3}$, where V_{di} are interatomic distances as defined in Fig. 1). In the bigger supercell, however, the threefold symmetry breaks and one interatomic distance (V_{d2}) is about 2% bigger than the two other distances. As a result, the four nearest neighbors of the vacancy make a pyramid that is elongated in the direction of the phosphorus atom with an isosceles triangle of Si atoms as a basis. The “center of mass” of this pyramid remains located in the vacant site of the original Si lattice in the case of PV⁺, but is shifted towards P by 3 and 2% –4% of Si interatomic distance for PV⁻ and PV⁰, respectively. It is interesting, however, that the distances between P and the silicon atoms in the pyramid remain equal to each other, constituting 3.80, 3.66, and 3.60 Å for PV⁺, PV⁰, and PV⁻, respectively.

In contrast, the relaxation of Si atoms in the group at the phosphorus side (Si_{Pi}) is symmetrical in both 64 and 216 atom supercells and occurs in the same direction as that of the P atom. The distances between Si_{Pi} atoms remain equal ($P_{d1} = P_{d2} = P_{d3}$) and shrink noticeably less than in the case of vacancy neighbors, due to the fact that the shift of the phosphorus atom is small and not too much different for different charge states. The relaxation of the Si_{Pi} atoms towards the vacant site is smaller than that of P atom and, as a result, the bond angles $Si_{Pi} - P - Si_{Pj}$ decrease by 2–3° as compared to the bulk silicon dihedral angle of 109°28', see Table III. Correspondingly, the angles of $Si_{Pi} - P$ bonds with the direction P–V increase by 2°–3° and reach 112°–113°, depending on the charge state.

The description of the relaxation of the second nearest neighbor shell to a PV pair can be conveniently done by dividing them into six three-atomic groups as shown in Fig. 2. Each such group consists of the nearest neighbors of an individual first neighbor of the complex. These groups are referred below as TV and TP, where T stands for “triangle,” while V and P indicate that the corresponding group is located at the vacancy or phosphorus side of a PV complex, respectively. The data related to the relaxation of atoms in TV and TP groups, are collected in Table IV. From the phos-

TABLE III. A summary of the relaxations for the nearest neighbors of the PV complex in different charge states. Pd and Vd are defined in Fig. 1, while ΔPd and ΔVd show the relative shrinkage of these values with respect to bulk Si interatomic distance (2.36 Å). $\Delta P-Si_p$ values represent the relative changes of distances between P atom and its nearest neighbours as compared to the corresponding distance in the bulk silicon (3.86 Å). Similarly, $\Delta V-Si_v$ defines relaxation of distances between the vacant site and its nearest silicon neighbours. For 64-atomic SC array the calculations predict completely symmetric relaxation. Therefore, there is only one number per cell for each charge state of E-center. In contrast, for 216-atomic SC all parameters are given for each charge state.

Complex	Pd1 Pd2 Pd3	$\Delta Pd(\%)$	$\Delta P-Si_p(\%)$	P-Si _p bond angle	Vd1 Vd2 Vd3	$\Delta Vd(\%)$	$\Delta V-Si_v(\%)$	V-Si _v bond angle
64 SC								
PV ⁺	3.72	-3.51	-2.2	107.4	3.64	-5.6	-4.2	107.07
PV ⁰	3.71	-3.86	-2.0	106.4	3.50	-9.1	-8.1	107.11
PV ⁻	3.71	-3.90	-2.0	106.4	3.38	-12.4	-11.2	107.27
216 SC								
	3.70	-4.0	-2.1	106.31	3.57	-5.1	-6.7	106.46
PV ⁺	3.70	-4.0	-2.0	106.32	3.64	-3.9	-4.4	107.30
	3.70	-4.0	-2.0	106.32	3.58	-3.8	-4.1	106.41
	3.70	-4.0	-2.1	106.30	3.58	-3.8	-4.1	106.41
PV ⁰	3.69	-4.3	-2.1	105.91	3.34	-8.2	-12.1	104.89
	3.69	-4.3	-2.0	105.88	3.52	-6.5	-9.4	110.34
	3.69	-4.3	-2.1	105.92	3.35	-6.4	-9.3	104.88
PV ⁻	3.69	-4.3	-2.1	105.83	3.26	-9.2	-14.2	105.63
	3.69	-4.3	-2.2	106.06	3.40	-7.9	-12.3	109.91
	3.69	-4.3	-2.1	105.84	3.26	-7.9	-12.2	105.48

phorus side, all the triangle groups from TP₁ to TP₃ follow the same relaxation pattern, namely shift towards phosphorus atom, two atoms (S_{P2} and S_{P3} in Fig. 2) shift outwards, while one atom (S_{P1}) can shift either inwards (similar to the nearest neighbors of the phosphorus atom), or outwards, depending on the charge of PV complex (see Table IV). As a result of these shifts the plane of a TP triangle “inclines” towards the vacant site.

The TV atom displacements are more sensitive to the choice of the charge state of the defect than those of phosphorus environment (Table IV). For these atoms a com-

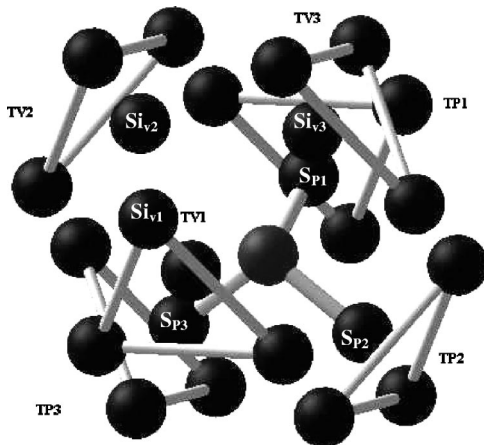


FIG. 2. Schematics of the atomic structure of the second coordination shell around a PV complex. Three-atomic groups connected by bonds and indexed as TV and TP include the second nearest neighbors for vacancy and phosphorus, respectively.

pletely inward relaxation for the PV⁰ and PV⁻ and partially outward one for PV⁺ takes place. In addition to the charge state, the relaxation pattern of TV groups is sensitive to the supercell size. This is directly related to the different symmetry of the vacancy first neighbor silicon atoms in 64 and 216 atom SC. It should be kept in mind that the displacements of atoms in the second neighbor shell are quite small, so the calculation provides rather a trend for the relaxation direction. Nevertheless, it is clear that the relaxation leads to the symmetry reduction for both TV and TP triangles. This is illustrated in the last two columns of Table IV, where we present dihedral angles formed by atoms of an individual TV/TP triangle with their common first neighbor of the PV complex (correspondingly, either Si_v or Si_p). In the case of 64-atom SC one can notice that at least two of these angles are equal. In the case of 216-atomic SC this trend holds only approximately and in some cases (e.g., TV₃ for charge state PV⁺) all three dihedral angles can be different.

B. Distribution of charge density around the PV complex

Bonding interactions can be classified on the basis of the position of the localized bonding domain along the bond path; the closer the position of the domain to the midpoint of the path, the greater the shared-electron interaction in a covalent bond. Figure 3 shows charge density variation along the lines connecting the first neighbors of a vacant site to the vacancy position. In case when phosphorus substitutes a Si atom, well-defined domains of increased electron density along the bonds connecting P to its three Si neighbors are observed. These domains are shifted to the phosphorus atom

TABLE IV. A summary of the relaxations for the second nearest-neighbors of a PV complex in different charge states. Second nearest neighbors are divided in three-atomic groups, so that atoms in each group are the nearest neighbors to one of the first nearest neighbor of the complex (see Fig. 2). Pd_i and Vd_i are distances between the members of the TP and TV groups, respectively (Fig. 2). ΔP and ΔV are the relative changes (relaxation) of distances between second neighbor atoms and a corresponding component of a VP pair, as compared to the Si bond distance in the bulk (3.86 Å). Bond angles are angles between the bonds between the atoms in a triangular group to the air common first neighbor of the PV pair.

	Vd(A)	Pd(A)	$\Delta V(\%)$			$\Delta P(\%)$	Bond angle (grad)			
Complex	TV ₁	TP ₁	S_{V1-V}	S_{V2-V}	S_{V3-V}^a	S_{P1-P}	$S_{V2-SiV-S_{V3}}$			$S_{P2-SiP-S_{P3}}$
	TV ₂	TP ₂					$S_{V2-SiV-S_{V1}}$			$S_{P2-SiP-S_{P1}}$
	TV ₃	TP ₃					$S_{V3-SiV-S_{V1}}$			$S_{P3-SiP-S_{P1}}$
64 SC										
PV ⁺	3.76	3.87	-0.1	-0.1	-2.0	-0.4	105.6	109.7		
	3.82	3.82	-0.1	-0.1	-2.0	0.7	109.3	106.8		
	3.82	3.87	-0.1	-0.1	-2.0	0.7	109.3	109.7		
PV ⁰	3.76	3.87	1.3	1.3	-0.3	-0.1	103.7	109.4		
	3.82	3.82	1.3	1.3	-0.3	0.7	106.9	106.8		
	3.82	3.87	1.3	1.3	-0.3	0.7	106.9	109.4		
PV ⁻	3.76	3.87	2.3	2.3	1.3	0.2	102.3	109.2		
	3.82	3.82	2.3	2.3	1.3	0.7	104.9	106.9		
	3.82	3.87	2.3	2.3	1.3	0.7	104.9	109.2		
216 SC ^a										
PV ⁺	3.87	3.86	1.2	-0.8	1.2	-0.4	109.6	105.6	110.0	109.6
	3.86	3.81	0.8	-0.9	0.7	0.7	109.8	105.8	109.2	106.4
	3.78	3.86	0.9	-0.9	0.7	0.7	108.7	104.3	108.7	109.5
PV ⁰	3.77	3.87	2.3	-0.2	2.3	0.2	104.6	102.8	107.4	109.3
	3.78	3.81	2.1	-0.3	0.3	0.7	104.7	102.9	107.5	106.4
	3.71	3.87	2.1	-0.3	0.3	0.7	105.6	101.2	105.5	109.6
PV ⁻	3.76	3.87	2.2	0.5	2.2	0.2	102.7	101.1	104.8	109.4
	3.76	3.81	2.2	0.1	0.5	0.7	102.8	101.1	104.9	106.4
	3.70	3.87	2.2	0.2	0.5	0.7	103.6	100.2	103.5	109.6

^aIn the case of 216-atomic SC triangle TV₁ is not identical to TV₂ and TV₃ due to the asymmetric deformation of Si first neighbors of the vacancy. Therefore, data in these cells of the table is presented as a set of three rows, corresponding to TV₁, TV₂, and TV₃, respectively.

and the displacement is quite big, therefore one can talk about the mixed ionic-covalent bond or, in other words, about polar covalent bond. The formation of a vacancy in the vicinity of the P atom results in a similar distribution of charge density near the phosphorus atom. It should be noted that the valence electrons not involved in the formation of bonding pairs remain localized close to the P ion (Fig. 3) and do not form domains protruding towards the vacant site (see Fig. 4).

In order to correctly specify the presence of a chemical bond, one has to consider pairing of electron spins in the overlapping electron orbitals from neighboring atoms. A convenient indirect tool, allowing us to estimate the presence of bonding on the basis of the same-spin electron density is provided by the electron localization function (ELF) approach.¹⁷ ELF provides a quantitative measure of “localization” of valence-electron pairs in appropriate regions of space of a given bond, or more generally of a given valence

region of the system. As it is known, ELF is a scalar function, conveniently ranging from zero to one, that uniquely identifies regions of space, where the electrons are well localized. Savin *et al.*¹⁷ formulated a meaningful physical interpretation: where ELF is close to its upper bound, electrons are strongly paired and the electron distribution has a local “bosonic” character. We show in Fig. 4 the charge density map in the (110) plane containing a phosphorus atom and a vacancy. Pseudoatoms correspond to the black regions, where ELF has a minimum value. In the bulk Si region, one clearly sees almost white regions in Fig. 4 between neighbor Si atoms, whose bonding pattern in this geometry has the shape of a “zig-zag” chain. In these bonding regions ELF attains the maximum value of 0.95. In agreement with the chemical picture of the covalent bond, we associate these regions with the opposite-spin electron pairs localized between each pair of bonded atoms.

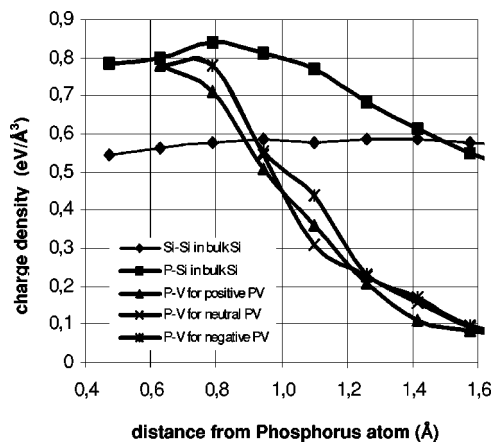


FIG. 3. Charge density change along the line connecting a vacant site to phosphorus in the 216-atom SC. Additionally charge density changes along a P-Si bond for substitution P atom and for Si-Si bond in bulk silicon are shown for comparison.

The distribution of the four maxima of electronic density around the phosphorus atom in the PV pair is consistent with the formation of sp^3 domains of localized electron density, corresponding to one nonbonding-electron and three bonded electron pair regions (Fig. 4). It is found that the heights of the maxima along the Si-P bonds are practically independent of the charge state of the PV complex and have very weak dependence on the length of Si-P bonds. As we can see in Fig. 3, there is a small displacement of the electron localization maximum towards the phosphorus ion due to the vacancy formation. It should be noted, however, that this is valid only for the 216-atom SC, while in the case of the 64-atom SC the electron localization maximum position along PV-bond is located farther from the P atom in comparison to substitutional P in a perfect silicon crystal. The maximum value of electron density in dangling bond region changes only moderately after vacancy formation ($0.84 e/\text{\AA}^3$ for substitutional P in perfect silicon crystal vs $0.78 e/\text{\AA}^3$ for the crystal with phosphorus-vacancy pair). Note that this value is nearly twice as high as the electron density in the region of a Si dangling bond in a pure silicon crystal with a vacancy, which is $\sim 0.34 e/\text{\AA}^3$ for positively charged vacancy and $\sim 0.4e/\text{\AA}^3$ for the neutral one. This indicates that a

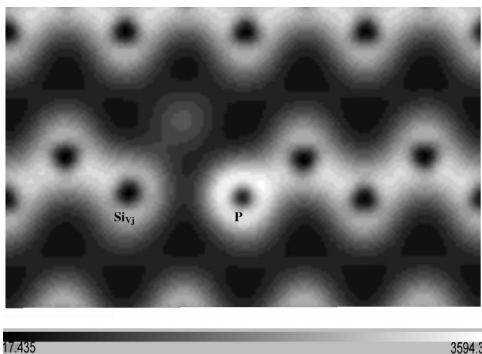


FIG. 4. Electron localization function map for the [110] plane, containing the phosphorus atom and vacancy for the case of the negatively charged PV complex.

well-localized lone pair is located close to phosphorus atom and the size of the localization region continuously shrinking with the increase of PV pair charge from positive to negative (see a shift of curves in Fig. 3). It is interesting to note that, for the system containing a vacancy, the charge density for other three P-Si_p bonds also decreases, most probably because of the elongation of these bonds. The patterns of charge density distribution for the silicon nearest neighbors (Si_{vj}) of the vacancy noticeably depend on the charge state of the complex (Fig. 5) and strongly correlate with the relaxation displacements. The position of the maximum of the electron density for the Si_{v1} strongly depends on the charge (Fig. 3). We found that the same is true for the position of ELF maximum. On the contrary, for two other neighbors the position of the maximum does not change with the charge of the pair. The values of ELF in the maximum change from 0.86 for PV⁺ to 0.9 for PV⁻. When the ELF value for the isosurface of the complex exceeds 0.86, the corresponding isosurface around Si_{vj} disappears as a single entity, showing no evidence for splitting into two different isosurfaces. Thus it indicates that the feature ascribed to nonbonding electrons is localized in a single domain, rather than in two well-defined domains.

In Fig. 5 the charge-density maps for the different charge states of PV complex are presented for the plane containing triangle Si_{v1}-Si_{v2}-Si_{v3}. A region of quite high charge density that connects Si_{v1}-Si_{v2}-Si_{v3} is found (Fig. 5). The maximum of the charge density in this region changes from $0.33 e/\text{\AA}^3$ up to $0.4 e/\text{\AA}^3$ depending on the charge state. This “connecting” region looks like a V-shape channel. The ELF map for the differently charged complexes presented in Fig. 6 shows the regions of the increased electron localization.

IV. DISCUSSION

The energetically most favorable charge state of the PV-complex depends on the position of the Fermi level in the band gap. According to our calculations, any of the three considered charge states can become energetically favorable under appropriate conditions, therefore below we consider in detail all of them.

Our calculations show that the relaxation of nearest neighbors of a PV complex occurs inwards (cf. Table III). This relaxation pattern is in agreement with that predicted in Ref. 12, obtained by Car-Parrinello molecular dynamics simulations¹³ and, in contrast, disagrees with predictions of outwards relaxation for PV⁰ and PV⁻ resulting from comparison of measured and theoretically calculated positron lifetimes.¹⁵ It should be noted, however, that the same controversy is met for an individual vacancy in silicon: positron lifetime experiments also predict outwards relaxation for the first neighbors of vacancy,¹⁵ while a host of recent calculations^{3,4,8} indicates the inward relaxation. The value of the inward shift of vacancy neighbors depends on the charge state: the more negative is the charge, the more compact is the structure of the complex. This can be interpreted as decreasing of the vacancy formation volume in transition from PV⁰ to PV⁻, which agrees with DLTS (Ref. 9) and positron lifetime^{10,11} experiments. The magnitude of inward relax-

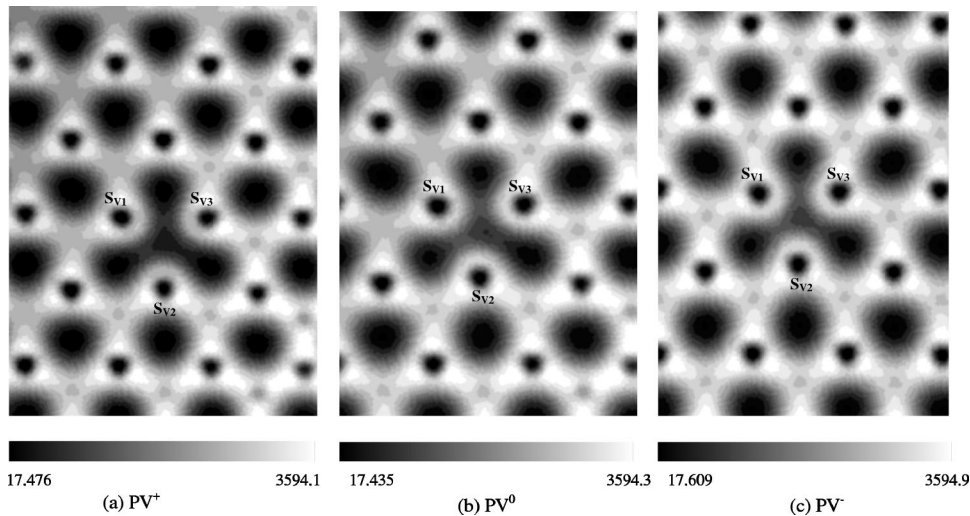


FIG. 5. Total charge density map in the vicinity of a PV complex in different charge states: (a) PV^+ , (b) PV^0 , (c) PV^- , cross section is made in planes containing Si_{V1} - Si_{V2} - Si_{V3} atoms.

ation of the nearest neighbors of the vacancy belonging to the PV complex is twice as large as that for the isolated vacancy. For example, similar *ab initio* calculations for a negative vacancy in Si (Ref. 8), predict inward relaxation of only 0.2 Å (or $\sim 5\%$ of a Si-Si bond).

Normally, a substitutional P atom, having before ionization five electrons (s^2p^3) in its outer electronic shell, is in the state P^+ , which means that one valence electron is donated to the conduction band, while the remaining four electrons provide bonding to the surrounding Si atoms. When a neutral vacancy is placed near a substitutional phosphorus atom (according to the reaction $P^+ + V^0 \Rightarrow PV^+$), the vacancy accommodates four uncompensated electrons at dangling bonds from surrounding atoms (that are P and Si_{Vj}). This situation resembles that encountered for a vacancy in pure Si, where also four uncompensated electrons are accommodated in the vacancy. However, the reconstruction of electronic configuration for PV^+ and for an isolated vacancy occurs completely differently. For the vacancy, the uncompensated electrons tend to form two pairwise connections (weak bonds) between the vacancy neighbors, leading to the so-called “pairing distortion” of the local vacancy environment.^{1,8} On the contrary, when one of the vacancy neighbors is a phosphorus atom, the latter tends to attract two of the available electrons and completely fills its outer electronic shell, transforming

itself to P^0 . Qualitatively the same scenario for phosphorus neutralization is observed also when phosphorus captures a negatively charged vacancy, resulting either in a neutral complex ($P^+ + V^- \Rightarrow PV^0$) or a negatively charged one ($P^+ + V^{2-} \Rightarrow PV^-$). The reason for such behavior of phosphorus can be readily seen in Fig. 3. Indeed, even for the case of a substitutional P^+ , the electronic density in a P-Si bond is shifted significantly toward P due to its higher electric charge (compare charge density distributions along Si-Si and P-Si bonds, squares and diamonds in Fig. 3, respectively). In the case when a Si atom in such a pair is replaced by a vacancy, the distribution of electron density close to P (in particular, the position and the height of the electron density maximum) remains practically unaffected, no matter what is the total charge of PV complex (compare charge distribution along PV lines in Fig. 3). On the other hand, closer to the vacant site the electron density drops quite sharply, which means more pronounced localization of an electron pair in the P-V direction accompanied, naturally, with a widening of the localization region transverse to this direction. The resulting pattern of the electron pair localization is nicely seen in Fig. 4 (for the case of PV^-), where no dangling bond is observed from the vacancy side of phosphorus atom. It is interesting that for a neutral PV complex a strong bonding of an electron pair to phosphorus atom was predicted experimentally al-

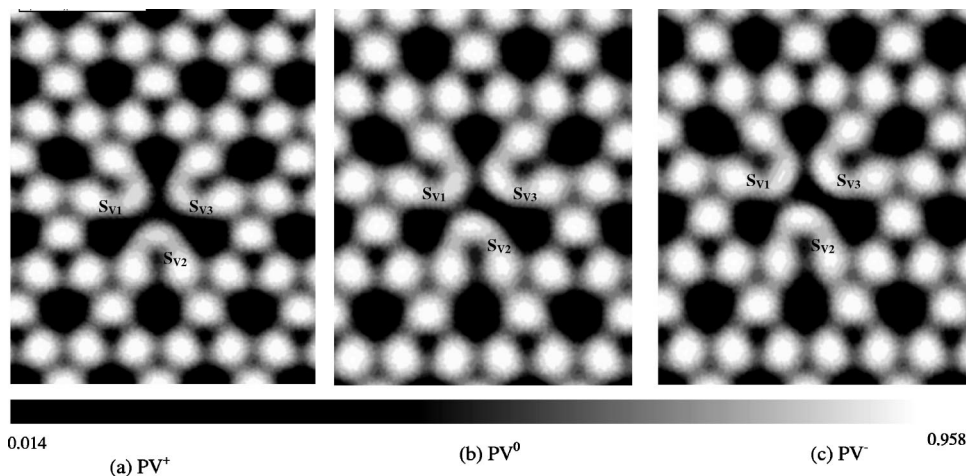


FIG. 6. Electron localization function map for the environment of the complex in different charge states: (a) PV^+ , (b) PV^0 , (c) PV^- , cross section is made in planes containing Si_{V1} - Si_{V2} - Si_{V3} atoms.

ready by Watkins and Corbett in Ref. 7. Our results are not only in good agreement with this finding, but predict the same type of electron spatial localization at the P atom for both charged configurations too, even for PV^+ .

As a result of phosphorus neutralization, there are from two (for PV^+) to four (for PV^-) uncompensated electrons in the vacancy, which have to be somehow redistributed in the triangle of remaining Si neighbors of the vacancy. At least three possibilities are available: (i) these electrons can be distributed in a fully symmetrical way, leading to the symmetric relaxation of Si triangle towards the vacant site, (ii) electrons can be shared by only two bonds in the triangle, which becomes isosceles triangle with a broad base (cf. Ref. 8), or (iii) at least one full bond can be formed, leading to the formation of isosceles triangle with a narrow base. It is interesting that case (iii), usually adopted as the basic model for electron density distribution between the Si neighbors of a vacancy in an E-center,⁷ is not observed in the present simulation. Only electron relaxation patterns (i) and (ii) are found, depending on the supercell size. This influence of the supercell size can possibly be related to the degree of structural relaxation of the lattice in the cell, imposed by purely computational restrictions, as discussed later in this section.

The nature of chemical bonding between Si_{V_j} atoms can be deduced on the basis of our calculations using the LSD approximation. In the case of the 64-atom supercell one can observe practically no channels of enhanced electron density connecting Si_{V_j} atoms, indicating the lack of direct bonding between these vacancy nearest neighbors. According to LSDA calculations for the PV^+ complex, two electrons have opposite spin and are distributed with equal probability among the three Si_{V_j} -atoms. Indeed, the integrals of the charge localized around each of three Si_{V_j} -atoms are approximately the same for both electron spins. In the case of PV^0 pair there are two individual electrons with the same spin, one of which is localized on an individual atom (Si_{V_1}), and another one is distributed between two other silicon atoms (Si_{V_2} and Si_{V_3}), while the third electron with an opposite spin is equally distributed between all three atoms. In the case of PV^- one observes three electrons having the same spin, each localized on individual Si atoms, plus an additional electron, equally shared between the three Si_{V_j} -atoms.

In the case of the 216-atom SC the bonding picture is more complicated. Namely, only two pairwise bonding connections remain between Si_{V_j} -atoms, while the local electron density between one pair of Si_{V_j} atoms disappears completely (in the discussion below we will refer to these atoms as Si_{V_2} and Si_{V_3}). This general pattern holds for all three considered charge states of the PV complex. However, the details differ quite significantly, depending on the charge state of the E-center.

As a result of the lattice relaxation after the formation of a positively charged E-center, the distances $Si_{V_1}-Si_{V_2}$ and $Si_{V_1}-Si_{V_3}$ become $\sim 1.6\%$ shorter than the distance $Si_{V_2}-Si_{V_3}$ (see Table III). Correspondingly, the symmetry of the tetrahedron formed by vacancy nearest neighbor atoms is reduced not only as compared to the tetrahedral symmetry of a site in the diamondlike lattice, but even as compared to the C_{2v} symmetry of a vacancy in Si, and includes only the mirror reflection with respect to (110) plane passing through

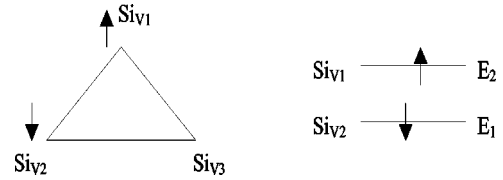


FIG. 7. Schematics of the resonant bond model for the PV^+ complex in silicon. Right-hand side represents the fueling of the electronic shells due to the bond formation between the Si_{V_j} atoms (see detailed description in the text).

P, V, and Si_{V_1} . In our opinion, the asymmetry of the observed configuration can be attributed to a manifestation of the Jahn-Teller effect,⁵ however of a special kind, first observed for a negatively charged divacancy in Si.⁸ Indeed, we have found that for the PV^+ complex the initial energy level splits into two new energy levels at ~ 0.18 eV (E_1) and ~ 0.3 eV (E_2) above the bottom of the band gap (see Fig. 7).

Since the phosphorus atom is neutralized and Si_{V_1} remains positively charged, the dangling one-electron orbitals are directed not to the vacant site, but rather toward Si_{V_1} , making a V-shaped “channel” that runs along the $Si_{V_2}-Si_{V_1}-Si_{V_3}$ path. The charge density distribution along the axis of this “channel” is presented in Fig. 5. For the PV^+ complex, two uncompensated electrons have different spins and are equally distributed along the “channel,” Fig. 5(a) and schematics in Fig. 7. In accordance with the observed spatial distribution of electron charge density, our calculation of a site-projected wave function indicates practically equal contributions associated with Si_{V_1} , Si_{V_2} , and Si_{V_3} vacancy neighbors ($\sim 24\%$ of the wave function) as well as to the density of states (DOS). However, for Si_{V_2} and Si_{V_3} the DOS maximum corresponds to the E_1 level, reaching the value of ~ 2.1 and 1.9 (for spins “up” and “down,” respectively, using units of “number of states/unit cell”), which is significantly bigger than that for the remaining level (~ 0.6 at each one). On the contrary, Si_{V_1} gives a noticeable contribution to the DOS at level E_2 (~ 1.7 and 2.0), but very small contribution (~ 0.8) at level E_1 . Combining DOS data with the data for partial charge density calculated for these energy levels we can propose an interpretation of electron distribution between levels as shown in Fig. 7. The low value of ELF (~ 0.5) indicates the lack of covalent bonds between Si_{V_j} atoms. At the same time, there is an equal probability to find an electron with spin “up” or “down” at an outer shell of any of Si_{V_j} atoms. The electron coming to Si_{V_2} or Si_{V_3} atom can occupy only E_1 level, whereas when it comes to Si_{V_1} it occupies E_2 energy level. Thus, we assume that bonding has a *resonant* character that occurs through the sequential change of the possible electronic configurations due to electron transitions between allowed energy levels. There are only few possible electronic configurations: (A) electron at Si_{V_2} (Si_{V_3})+electron at Si_{V_1} ; (B) two electrons at Si_{V_2} (Si_{V_3}); (C) electron at Si_{V_2} +electron at Si_{V_3} . Keeping this in mind and taking into account the data for ELF and the value of charge localized at Si_{V_j} atoms, we can ascribe a “resonant” mode to electron transitions (Fig. 7). Let us consider configuration (A) as an initial one. For this configuration, as mentioned above, one electron is at the E_1 level and another one is at the

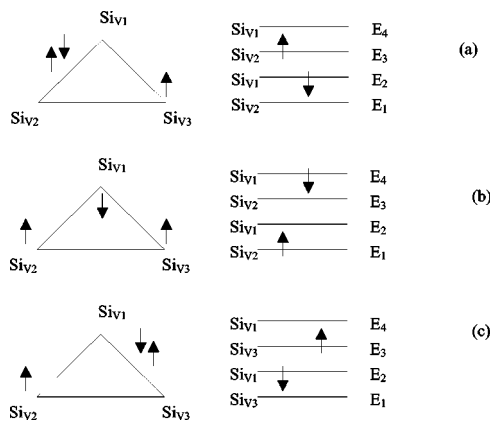


FIG. 8. Schematics of the resonant bond model for the PV^0 complex in silicon. Right-hand side represents the fueling of the electronic shells due to the bond formation between the Si_{V_j} atoms (see detailed description in the text).

E_2 level. Because the electron at E_2 level tends to decrease its energy, it moves from the Si_{V1} to Si_{V2} atom leading to configuration (B). This configuration is negatively charged, which is energetically unfavorable, and one electron moves from the atom to the next one along the V-channel (Si_{V2} - Si_{V1} transition) increasing its energy from E_1 up to E_2 . Further a double transition takes place: Si_{V2} - Si_{V1} for the electron being at Si_{V2} and Si_{V1} - Si_{V3} for the electron being at Si_{V1} (or E_1 - E_2 and E_2 - E_1) and the cycle repeats again.

For PV^0 the presence of three uncompensated electrons does not lead to the formation of purely symmetric relaxation pattern with three non-overlapping dangling bonds, but makes the V-shaped “channel” even more pronounced [Fig. 5(b)]. The charge density distribution indicates strong localization of the electrons of the same spin near Si_{V2} and Si_{V3} atoms. The third electron has, however, the opposite spin and is localized mainly in the vicinity of Si_{V1} , but contributes in equal shares to the formation of Si_{V1} - Si_{V2} and Si_{V1} - Si_{V3} bonds, as schematically shown in Fig. 8. The values of the ELF along the bonds (~ 0.82) allow to interpret these bonds as covalent ones. In such a situation, a symmetrical distribution of the partially filled orbitals at Si_{V_j} -atoms would result in a degeneracy, which can be removed by a spontaneous Jahn-Teller-type distortion of the triangle of Si_{V_j} -atoms. Indeed, we have found that for the PV^0 complex the initial energy level splits into four sublevels: two levels that have already been found for PV^+ at ~ 0.18 eV (E_1), ~ 0.3 eV (E_2), and two additional levels at ~ 0.34 eV (E_3) and 0.4 eV (E_4) above the bottom of the band gap (see Fig. 8). The charge density localized in the vicinity of Si_{V2} and Si_{V3} atoms has been found to be distributed between E_1 and E_4 , while for Si_{V1} it is distributed between E_2 and E_3 . At the same time, for Si_{V2} and Si_{V3} atoms DOS maxima for the electrons having spins “up” and “down” correspond to E_1 and E_4 , respectively, which are more than two times bigger than for the other two levels. In contrast, Si_{V1} gives noticeable contribution to DOS at levels E_3 and E_2 for “up” and “down” electrons, respectively. Consequently, we suggest that the distribution of electrons in PV^0 between the split energy levels can be described as shown in Fig. 8.

The type of bonding observed in the PV^0 complex is quite interesting. Indeed, normally a chemical bond involves pairing of two opposite spin electrons, while in the considered case the bonding is provided by only one electron at Si_{V1} , which is shared by both bonds in the V-shaped channel. Such kind of bonding was suggested by Saito and Oshiyama for a divacancy in silicon⁸ and was interpreted as a “resonant bond” structure. Similarly, Seong and Lewis found the resonant type distortion for the neutral divacancy in silicon.¹⁸ Even more interesting, that more recent *ab initio* calculations of Pesola *et al.*, performed using a 216-atom SC, showed the changing of bonding type from more of pairing type to more of resonant type distortion in going from positively to negatively charged divacancy.³ For a simple qualitative picture allowing to rationalize the resonant type of bonding for the PV^0 complex, one can assume that the electron at Si_{V1} “switches” between the bonds at sufficiently high frequency (Fig. 8). If we assume that the energy level E_4 corresponds to an electron localized at Si_{V1} , then it is energetically favorable for this electron to decrease its energy down to E_2 by forming a pair with an electron from one of the other two Si_{V_j} atom, even though the latter electron will have to jump from E_1 up to E_3 as well. On the other hand, if this configuration dissociates and the antispin electron returns to Si_{V1} , a new bond can be created with another silicon atom, since Si_{V2} and Si_{V3} are completely equivalent. This “resonant” formation-dissociation of bonds (represented, on the average, as equipartition of the electron density at Si_{V1} between two bonds) allows us to stabilize the whole triangle of Si_{V_j} atoms at closer distances than those in the ideal lattice, but does not create a strong localized bond between any pair of Si_{V_j} -atoms, which would require much stronger distortion of the surrounding Si lattice.

Finally, let us consider what happens when one more electron is added to a vacancy-phosphorus pair, resulted in a PV^- complex. The LSDA calculations indicate that in this case three unpaired electrons have the same spin and are localized each at its own Si_{V_j} atom. The fourth electron has the opposite spin and is completely delocalized along the V-channel, so that the electron distribution among Si_{V_j} -atoms can be schematically represented as in Fig. 9. The total electron density distribution between Si_{V_j} -atoms [Fig. 5(c)] has the same V-shaped spatial arrangement, like that for PV^+ and PV^0 , and the variation of the total electron density along the channel axis is shown in Fig. 4. The energy level for the unpaired electrons splits into several levels, similar to that found for PV^+ and PV^0 , indicating that the Jahn-Teller symmetry breaking distortion occurs also for PV^- . However, for the negative charge state, the initial E_1 level splits into two sublevels: at 0.15 eV (E_{1d}) and 0.2 eV (E_{1u}); E_2 has its original position; initial E_3 and E_4 levels are presented as one level at 0.37 eV (E_{3c}) and there are two additional levels at ~ 0.47 eV (that can be interpreted as a transition level) and ~ 0.63 eV (E_4). The distribution of electrons over the energy levels has been estimated using corresponding partial charge density values, which shows that electrons localized at the Si_{V2} (Si_{V3}) atom can occupy E_{1d} , E_{1u} , and E_{3c} levels, whereas electrons localized at the Si_{V1} -atom can be distributed between levels E_{1u} , E_2 , and E_4 . The analysis of the partial charge density distribution and site-projected density

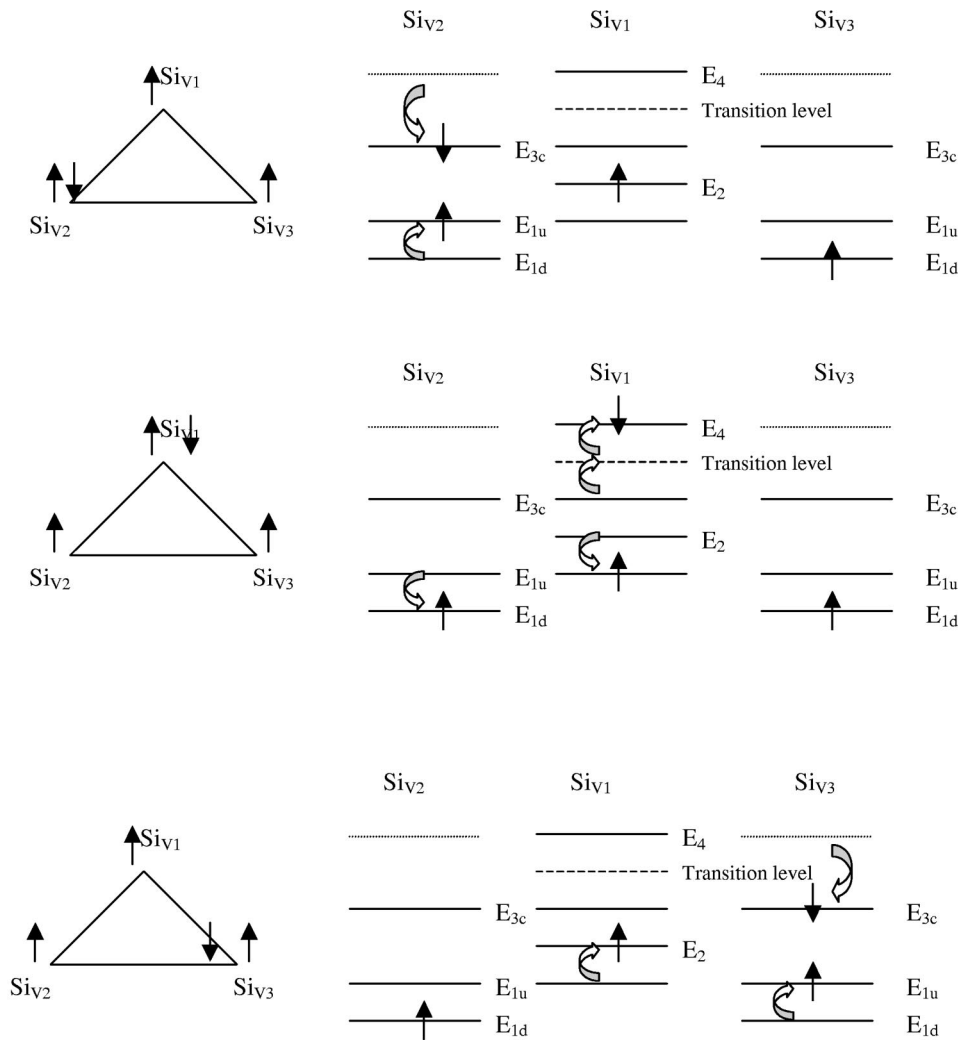


FIG. 9. Schematics of the resonant bond model for the PV^0 complex in silicon. Right-hand side represents the fueling of the electronic shells due to the bond formation between the Si_{V_j} atoms (see detailed description in the text).

of states calculated for the different spins allows us to interpret the bonding as presented schematically in Fig. 9.

As schematically shown in Fig. 9(a), the initial position of the electron localized at the Si_{V_2} is at the E_{1d} level. When a delocalized electron comes to the Si_{V_2} atom, it occupies E_{3c} level, while the localized electron shifts from E_{1d} to E_{1u} . At the same time, in this emerging electronic configuration, an electron localized at the Si_{V_1} atom occupies E_2 level, whereas an electron at the Si_{V_3} atom is at the E_{1d} level. Because the electron at Si_{V_2} tends to decrease its energy, this electronic configuration is metastable and the localized electron returns from E_{1u} to E_{1d} level that is accompanied by the transition of the delocalized electron from E_{3c} to the transition level that belongs to the Si_{V_1} atom [Fig. 9(b)]. This transition of the delocalized electron to the Si_{V_1} atom leads to a perturbation of the outer shell electron of this atom and results in the transition of the localized electron from E_2 to E_{1u} level, which accompanies a transition of the delocalized electron from the transition level to the E_4 level. In order to minimize the energy, this configuration dissociates through the delocalized electron transition from Si_{V_1} to Si_{V_3} atom, making electronic configuration similar to that presented in Fig. 9(a) [see Fig. 9(c)].

At this stage it seems reasonable to compare our findings with the experimental electron paramagnetic resonance

(EPR) results of Watkins and Cobett,¹ where the weak covalent bonding of two Si vacancy neighbors plus a dangling orbital pointing to the vacant site at the remaining one was chosen ad hoc as a working scheme for the rationalization of experimental observations. It can be seen that even though this particular model is not confirmed by our results, the symmetry of the vacancy environment [that is a unique reflection plane of type (110) through phosphorus, vacancy and one of Si_{V_j} -atoms] in the case of the 216-atom SC is exactly the same as that in the original model of Watkins and Corbett. The origin of the symmetry reduction is in both cases the Jahn-Teller-type distortion, even though the nature of resulting bonding in the two models is completely different. Correspondingly, the finding that “an additional electron can be accommodated at ($E_c - 0.4$ eV)” (where E_c is the bottom of conduction band) can be reasonably correlated to the presence of a level at energy E (Fig. 8): having in mind that the band gap in Si is close to 1.12 eV (see, e.g., Ref. 19). Also, the distribution of electrons among the possible sub-levels conforms to the experimental requirement that this level must be free of electrons in order to allow the EPR detection of an unpaired electron bound to one of the Si vacancy neighbors in a neutral E-center.¹ As it has been shown there is a principal difference between the results ob-

tained using 216-atom and 64-atom SC calculations. In contrast to the 216-atom SC calculations as well as to the experimental observations, the results for 64-atom SC do not predict either asymmetry of Si_{V_j} -atoms, or Jahn-Teller energy level splitting, independent of the charge of the PV-complex. The reason for that is not quite clear, especially having in mind that the resonant-bond distortion was observed in the same supercell for a divacancy,⁸ which is characterized by much less inward relaxation of divacancy's nearest neighbors and thus by even bigger distances between Si atoms participating in the resonant bonds, as compared to our calculations. One possible reason can be the restrictions imposed by the limited system size. Indeed, as can be seen from Table IV, the symmetry reducing distortion of the vacancy first neighbor configuration is accompanied with more pronounced outward relaxation of some atoms in the second nearest neighbor shell, as compared to purely symmetric relaxation, and may be hindered by more restrictive boundary conditions in the 64-atom SC compared to the 216-atom one. As a result, even in the case of the strongest relaxation (for PV^-) the distance between Si_{V_j} -atoms remains larger than the threshold for the overlap of electron clouds of neighboring atoms (according to the results of Table IV, this threshold distance falls somewhere in the range from 3.35 to 3.38 Å). This means that at least five coordination shells around a defect are to be taken into account in calculations in order to get more or less realistic results for electronic structure and energetic characteristics of a defect. Thus it is reasonable to assume that the results of the 216-atom SC calculation are more realistic than those with smaller SC, and a resonance-type bonding takes place for the PV center as predicted by these calculations.

V. CONCLUSIONS

Based on the results of our *ab initio* calculations of the structural and electronic relaxation of phosphorus-vacancy pair in Si in three different charge states, we draw the following conclusions:

(1) The first nearest-neighbors of the PV complex relax inwards for all charge states, while the relaxation pattern of the second nearest-neighbors depends on both the charge state and the size of the supercell. The degree of relaxation increases as the charge changes from positive to negative.

(2) The phosphorus atom is found to capture two electrons and shift exactly in the direction of the vacant site for all PV configurations, which is in agreement with experimental observations in Ref. 7.

(3) The relaxation pattern of the Si neighbors of the vacancy depends on a supercell size. In the bigger 216-atom SC the asymmetric relaxation is found, in accordance with the experimental results of Ref. 7. The nature of the symmetry obtained in the present electronic structure calculations is completely different from that postulated in Ref. 7 as a "pairing distortion," and is similar to "resonant"-type suggested in Ref. 8. The features of the level occupation are found to be sensitive to the charge state of the PV complex.

ACKNOWLEDGMENTS

This research was supported by Wenner-Gren Center and the Nordic Academy for Research Training. We wish to thank the Center for Scientific Computing (Helsinki, Finland) and Norwegian University of Science and Technology (Norway) for the use of their computational facilities.

¹G. D. Watkins, in *Deep Centers in Semiconductors* (Gordon and Breach, New York, 1986), p. 147.

²G. D. Watkins and J. W. Corbett, *Phys. Rev.* **138**, A555 (1965).

³M. Pesola, J. Von Boehm, S. Pöykkö, and R. M. Nieminen, *Phys. Rev. B* **58**, 1106 (1998).

⁴M. J. Puska, S. Pöykkö, M. Pesola, and R. M. Nieminen, *Phys. Rev. B* **58**, 1318 (1998).

⁵H. A. Jahn and E. Teller, *Proc. R. Soc. London, Ser. A* **A161**, 220 (1937).

⁶G. D. Watkins and J. W. Corbett, *Phys. Rev.* **138**, A543 (1965).

⁷G. D. Watkins and J. W. Corbett, *Phys. Rev.* **134**, A1359 (1964).

⁸M. Saito and A. Oshiyama, *Phys. Rev. Lett.* **73**, 866 (1994); O. Sugino and A. Oshiyama, *ibid.* **68**, 1858 (1992).

⁹G. A. Samara, *Phys. Rev. B* **37**, 8523 (1988).

¹⁰J. Mäkinen, P. Hautojärvi, and C. Corbel, *J. Phys.: Condens. Mat-*

ter **4**, 5137 (1992).

¹¹J. Mäkinen, C. Corbel, P. Hautojärvi, P. Moser, and F. Pierre, *Phys. Rev. B* **39**, 10 162 (1989).

¹²R. Virkkunen and R. M. Nieminen, *Comput. Mater. Sci.* **1**, 351 (1993).

¹³R. Car and M. Parinello, *Phys. Rev. Lett.* **55**, 2471 (1985).

¹⁴J. Mäkinen and M. J. Puska, *Phys. Rev. B* **40**, 12 523 (1989).

¹⁵M. J. Puska, *J. Phys.: Condens. Matter* **3**, 3455 (1991).

¹⁶O. Gunnarsson, B. L. Lundqvist, and J. W. Wilkins, *Phys. Rev. B* **10**, 1319 (1974).

¹⁷A. Savin, A. D. Becke, J. Flad, R. Nesper, H. Preuss, and H. G. v. Schnering *Angew. Chem., Int. Ed. Engl.* **30**, 409 (1991).

¹⁸H. Seong and L. J. Lewis, *Phys. Rev. B* **53**, 9791 (1996).

¹⁹P. J. Collings, *Am. J. Phys.* **48**, 197 (1980).